THE STRUCTURAL DESIGN OF TALL AND SPECIAL BUILDINGS
Struct. Design Tall Spec. Build. **18**, 203–216 (2009)
Published online 9 October 2007 in Wiley Interscience (www.interscience.wiley.com). **DOI**: 10.1002/tal.405

IDENTIFICATION OF MODAL DAMPING RATIOS OF FOUR-FLUE CHIMNEY OF A THERMOELECTRICAL PLANT USING PSEUDO-INVERSE MATRIX METHOD

M. CAVACECE[1], P. P. VALENTINI[2] AND L. VITA[2]*
[1] *Department of Structural Engineering—DIMSAT, University of Cassino, Cassino, Italy*
[2] *Department of Mechanical Engineering, University of Rome, Rome, Italy*

SUMMARY

Some computational issues related to the identification of modal parameters of structures are presented in this paper. Optimal estimation of modal parameters often requires the solution of an overdetermined linear system of equations. Hence the computation of a pseudo-inverse matrix is involved. In this paper the numerical performance of different algorithms for Moore–Penrose pseudo-inverse computation have been tested for modal analysis of a four-flue chimney of a thermoelectrical plant. The computational scheme herein adopted for parameter identification is based on well-known modal properties and has a fast rate of convergence to solution. The computation of the Rayleigh damping coefficients α and β is an important step in the area of the modal superposition technique. The proposed approach can accurately predict damping ratios and all the eigenvectors without evaluating mass and stiffness matrices. Copyright © 2007 John Wiley & Sons, Ltd.

1. INTRODUCTION

Recently analytical and experimental modal analysis, or vibration system identification, has become an increasingly popular technique. Developments in measuments have facilitated the acquisition of reliable experimental data. These procedures lead to extraction of the modal properties of a test structure (Ewins and Gleeson, 1982; Luk, 1987; Lagomarsino, 1993; Watanate *et al*., 1997; Mohammad *et al*., 1995; Dovstam, 1997; Prells and Friswell, 2000; Adhikari and Woodhouse, 2001; Gaylard, 2001; Liu *et al*., 2001; Lee *et al*., 2004; He and Fu, 2004; Trombetti and Silvestri, 2006). The building response to dynamic excitation, such as wind or earthquake, can be evaluated using techniques such as the direct integration of equations of motion to modal analysis or the use of response spectra. In each case the availability of the stiffness, inertia and dissipative parameters is very important.

The objective of this paper is to test different methods for the numerical computation of the pseudo-inverse matrix and to discuss their applicability in structural dynamics applications. The generalized inverse is a well-known tool in modern linear matrix theory. It is usually used to solve a set of over-determined or undetermined simultaneous equations (To and Ewins, 1995) through the application of the least squares optimization criterion. As a numerical test, by means of the proposed method the modal damping ratios and the modal shape of a chimney have been estimated assuming Rayleigh damping.

* Correspondence to: Leonardo Vita, Department of Mechanical Engineering, University of Rome, Tor Vergata, Via del Politecnico, Rome, 1-00133, Italy. E-mail: vita@ing.uniroma2.it

In the first two sections the basic equations used for the mathematical setting of the identification problems are briefly deduced. The third section is dedicated to reviewing different approaches for computing the Moore–Penrose pseudo-inverse matrix. In the fourth section the numerical results for different cases are discussed.

2. FUNDAMENTAL EQUATIONS OF STRUCTURAL DYNAMICS

The equations of motion (Singiresu and Rao, 2004) of a linear viscous damped multi-degree-of-freedom system in matrix form are

$$[m]\{\ddot{y}\}+[c]\{\dot{y}\}+[k]\{y\}=\{F(t)\} \tag{1}$$

By means of Laplace transformation of the response canonical equations of modal motion (de Silva, 2000) assuming zero initial conditions, one obtains the transfer function

$$H(s)=\sum_{r=1}^{N_r} H_r(X_iX_k)_r=\sum_{r=1}^{N_r}\frac{(X_iX_k)_r}{[s^2+2\zeta_r\omega_r s+\omega_r^2]} \tag{2}$$

between the excitation at the kth location and response at the ith location. Assuming Rayleigh damping, the damping matrix could be expressed as a linear combination of the mass and stiffness matrices

$$[c]=\alpha[m]+\beta[k] \tag{3}$$

This type of damping is known as proportional damping. This condition is sufficient to decouple the equations of motion (1), allowing the use of modal analysis. By means of equation (3) one obtains

$$\alpha+\omega_r^2\beta=2\zeta_r\omega_r \tag{4}$$

From

$$\omega_{d_r}=\omega_r\sqrt{1-\zeta_r^2} \tag{5}$$

equation (4) becomes

$$\alpha+\omega_r^2\beta=2\sqrt{\omega_r^2-\omega_{E_{r,q}}^2} \tag{6}$$

where $\omega_{d_r}=\omega_{E_{r,q}}$ with $\omega_{E_{r,q}}$ the experimental circular frequency of damped oscillation, obtained from the qth measurement and rth vibration mode.

3. IDENTIFICATION OF MODAL PARAMETERS

The equations deduced in the previous sections constitute the main blocks of the method for the identification of modal parameters (Figure 1). In this section their use for such purpose is presented.

Since the mathematical approach adopted is essentially a least squares solution of a redundant system of linear equations, from our treatment nonlinear equations are excluded.

DOI: 10.1002/tal

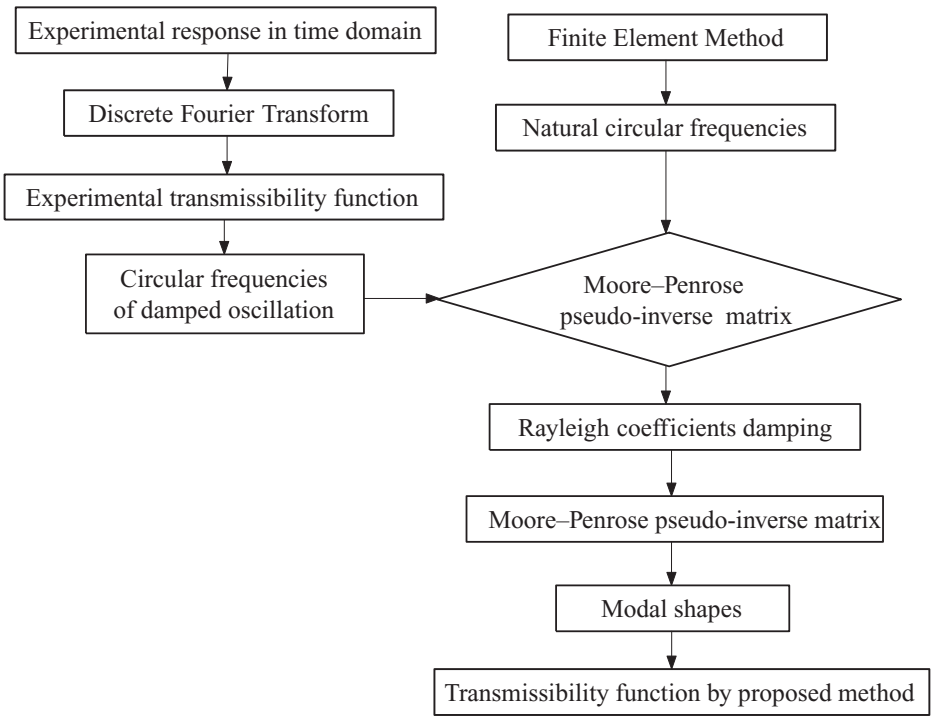

Figure 1. Flow chart of the method for identification of modal parameters

3.1 Rayleigh damping

From equation (6), the following system can be obtained:

$$\begin{bmatrix} 1 & \omega_1^2 \\ 1 & \omega_1^2 \\ \vdots & \\ 1 & \omega_1^2 \\ \vdots & \\ 1 & \omega_r^2 \\ 1 & \omega_r^2 \\ \vdots & \\ 1 & \omega_r^2 \\ \vdots & \\ 1 & \omega_{N_r}^2 \\ 1 & \omega_{N_r}^2 \\ \vdots & \\ 1 & \omega_{N_r}^2 \end{bmatrix} \begin{Bmatrix} \alpha \\ \beta \end{Bmatrix} = \begin{Bmatrix} 2\sqrt{\omega_1^2 - \omega_{E_{1,1}}^2} \\ 2\sqrt{\omega_1^2 - \omega_{E_{1,2}}^2} \\ \vdots \\ 2\sqrt{\omega_1^2 - \omega_{E_{1,N_q}}^2} \\ \vdots \\ 2\sqrt{\omega_2^2 - \omega_{E_{r,1}}^2} \\ 2\sqrt{\omega_2^2 - \omega_{E_{r,2}}^2} \\ \vdots \\ 2\sqrt{\omega_2^2 - \omega_{E_{r,N_q}}^2} \\ \vdots \\ 2\sqrt{\omega_3^2 - \omega_{E_{N_r,1}}^2} \\ 2\sqrt{\omega_3^2 - \omega_{E_{N_r,2}}^2} \\ \vdots \\ 2\sqrt{\omega_3^2 - \omega_{E_{N_r,N_q}}^2} \end{Bmatrix} \tag{7}$$

DOI: 10.1002/tal

for $q = 1, 2, \ldots, N_q$ and mode $r = 1, 2, \ldots, N_r$. By applying the least-squares optimality criterion, the redundant $N_q \times N_r$ equations system (7) is solved with respect to constants α and β. In this phase computation of the Moore–Penrose pseudo-inverse matrix has its main role.

3.2 Transmissibility function

From equation (2), $\lambda_1 = (2\pi f_1)^2$, $\lambda_2 = (2\pi f_2)^2, \ldots, \lambda_r = (2\pi f_r)^2, \ldots, \lambda_{Nr} = (2\pi f_{N_r})^2$ the square of the eigenvalues, the real component $\Re[H_{ik}(f)]$ of the transmissibility function at response location $\imath$ and excitation location k of the chimney is

$$\Re[H_{ik}(f)] = \frac{\dfrac{(X_iX_k)_1}{\lambda_1}\left[1-\left(\dfrac{f}{f_{d_1}}\right)^2\right]^2}{\left[1-\left(\dfrac{f}{f_{d_1}}\right)^2\right]^2+\left(2\zeta_1\dfrac{f}{f_{d_1}}\right)^2} + \frac{\dfrac{(X_iX_k)_2}{\lambda_2}\left[1-\left(\dfrac{f}{f_{d_2}}\right)^2\right]^2}{\left[1-\left(\dfrac{f}{f_{d_2}}\right)^2\right]^2+\left(2\zeta_2\dfrac{f}{f_{d_2}}\right)^2} + \cdots + \frac{\dfrac{(X_iX_k)_r}{\lambda_r}\left[1-\left(\dfrac{f}{f_{d_r}}\right)^2\right]^2}{\left[1-\left(\dfrac{f}{f_{d_r}}\right)^2\right]^2+\left(2\zeta_r\dfrac{f}{f_{d_r}}\right)^2} + \ldots + \frac{\dfrac{(X_iX_k)_{N_r}}{\lambda_{N_r}}\left[1-\left(\dfrac{f}{f_{d_{N_r}}}\right)^2\right]^2}{\left[1-\left(\dfrac{f}{f_{d_{N_r}}}\right)^2\right]^2+\left(2\zeta_{N_r}\dfrac{f}{f_{d_{N_r}}}\right)^2} \tag{8}$$

The imaginary component $\Im[H_{ik}(f)]$of the transmissibility function at response location i and excitation location k of the chimney is

$$\Im[H_{ik}(f)] = \frac{\dfrac{(X_iX_k)_1}{\lambda_1}\left(-2\zeta_1\dfrac{f}{f_{d_1}}\right)}{\left[1-\left(\dfrac{f}{f_{d_1}}\right)^2\right]^2+\left(2\zeta_1\dfrac{f}{f_{d_1}}\right)^2} + \frac{\dfrac{(X_iX_k)_2}{\lambda_2}\left(-2\zeta_2\dfrac{f}{f_{d_2}}\right)^2}{\left[1-\left(\dfrac{f}{f_{d_2}}\right)^2\right]^2+\left(2\zeta_2\dfrac{f}{f_{d_2}}\right)^2} + \cdots + \frac{\dfrac{(X_iX_k)_r}{\lambda_{N_r}}\left(-2\zeta_{N_r}\dfrac{f}{f_{d_r}}\right)}{\left[1-\left(\dfrac{f}{f_{d_r}}\right)^2\right]^2+\left(2\zeta_r\dfrac{f}{f_{d_r}}\right)^2} + \ldots + \frac{\dfrac{(X_iX_k)_{N_r}}{\lambda_{N_r}}\left(-2\zeta_{N_r}\dfrac{f}{f_{d_{N_r}}}\right)}{\left[1-\left(\dfrac{f}{f_{d_{N_r}}}\right)^2\right]^2+\left(2\zeta_{N_r}\dfrac{f}{f_{d_{N_r}}}\right)^2} \tag{9}$$

The modulus of the transmissibility function is then

$$H_{ik}(f) = \sqrt{\Re[H_{ik}(f)]^2 + \Im[H_{ik}(f)]^2} \tag{10}$$

From equations (8) and (9) with $f = \hat{f}_1, \hat{f}_2, \ldots, \hat{f}_{N_p}$, the following system can be obtained:

$$[A]\{X\} = \{b\} \tag{11}$$

DOI: 10.1002/tal

with

$$[A]=\begin{bmatrix} \dfrac{\frac{1}{\lambda_1}\left[1-\left(\frac{\hat{f}_1}{f_{d_1}}\right)^2\right]^2}{\left[1-\left(\frac{\hat{f}_1}{f_{d_1}}\right)^2\right]^2+\left(2\zeta_1\frac{\hat{f}_1}{f_{d_1}}\right)^2} & \cdots & \dfrac{\frac{1}{\lambda_{N_r}}\left[1-\left(\frac{\hat{f}_1}{f_{d_{N_r}}}\right)^2\right]^2}{\left[1-\left(\frac{\hat{f}_1}{f_{d_{N_r}}}\right)^2\right]^2+\left(2\zeta_{N_r}\frac{f}{f_{d_{N_r}}}\right)^2} \\ \dfrac{\frac{1}{\lambda_1}\left(-2\zeta_1\frac{\hat{f}_2}{f_{d_1}}\right)}{\left[1-\left(\frac{\hat{f}_2}{f_{d_1}}\right)^2\right]^2+\left(2\zeta_1\frac{\hat{f}_2}{f_{d_1}}\right)^2} & \cdots & \dfrac{\frac{1}{\lambda_{N_r}}\left(-2\zeta_{N_r}\frac{\hat{f}_2}{f_{d_{N_r}}}\right)}{\left[1-\left(\frac{\hat{f}_2}{f_{d_{N_r}}}\right)^2\right]^2+\left(2\zeta_{N_r}\frac{f_2}{f_{d_{N_r}}}\right)^2} \\ \vdots & \vdots & \vdots \\ \dfrac{\frac{1}{\lambda_1}\left(-2\zeta_1\frac{\hat{f}_p}{f_{d_1}}\right)}{\left[1-\left(\frac{\hat{f}_p}{f_{d_1}}\right)^2\right]^2+\left(2\zeta_1\frac{\hat{f}_p}{f_{d_1}}\right)^2} & \cdots & \dfrac{\frac{1}{\lambda_{N_r}}\left(-2\zeta_{N_r}\frac{\hat{f}_p}{f_{d_{N_r}}}\right)}{\left[1-\left(\frac{\hat{f}_{N_p}}{f_{d_{N_r}}}\right)^2\right]^2+\left(2\zeta_{N_r}\frac{\hat{f}_p}{f_{d_{N_r}}}\right)^2} \\ \vdots & \vdots & \vdots \\ \dfrac{\frac{1}{\lambda_1}\left(-2\zeta_1\frac{\hat{f}_{N_p}}{f_{d_1}}\right)}{\left[1-\left(\frac{\hat{f}_{N_p}}{f_{d_1}}\right)^2\right]^2+\left(2\zeta_1\frac{\hat{f}_{N_p}}{f_{d_1}}\right)^2} & \cdots & \dfrac{\frac{1}{\lambda_{N_r}}\left(-2\zeta_{N_r}\frac{\hat{f}_{N_p}}{f_{d_{N_r}}}\right)}{\left[1-\left(\frac{\hat{f}_{N_p}}{f_{d_{N_r}}}\right)^2\right]^2+\left(2\zeta_{N_r}\frac{\hat{f}_{N_p}}{f_{d_{N_r}}}\right)^2} \end{bmatrix} \tag{12}$$

$$\{b\}=\begin{Bmatrix} \Re\left[H_{ik}\left(\hat{f}_1\right)\right] \\ \Im\left[H_{ik}\left(\hat{f}_2\right)\right] \\ \vdots \\ \Im\left[H_{ik}\left(\hat{f}_p\right)\right] \\ \vdots \\ \Im\left[H_{ik}\left(\hat{f}_{N_p}\right)\right] \end{Bmatrix}, \{X\}=\begin{Bmatrix} (X_iX_k)_1 \\ (X_iX_k)_2 \\ \vdots \\ (X_iX_k)_r \\ \vdots \\ (X_iX_k)_{N_r} \end{Bmatrix} \tag{13}$$

By applying the least-squares optimality criterion, the redundant $N_p \times N_r$ equations system (11) is solved with respect to constants $(X_iX_k)_1$, $(X_iX_k)_2$, . . . , $(X_iX_k)_r$, . . . , $(X_iX_k)_{N_r}$. In this phase computation of the Moore–Penrose pseudo-inverse matrix has its main role.

4. THE MOORE–PENROSE PSEUDO-INVERSE MATRIX

This section, for completeness, summarizes the main properties of the Moore–Penrose pseudo-inverse matrix and the steps of the different algorithms tested during the dynamic simulations [18].

DOI: 10.1002/tal

4.1 Definitions

The main properties of the Moore–Penrose pseudo-inverse matrix $[A]^+$ of a matrix $[A]$ are

- $([A][A]^+)^T = [A][A]^+$
- $([A]^+[A])^T = [A]^+[A]$
- $[A][A]^+[A] = [A]$
- $[A]^+[A][A]^+ = [A]^+$

When $[A]$ is a square matrix with full rank, then its pseudo-inverse coincides with the inverse. The Moore–Penrose pseudo-inverse matrix is associated with the least-squares solution of the linear system of equations

$$[A]\{x\} = \{b\} \tag{14}$$

where the number m of equations is not equal to the number n of unknowns and $[A]$ does not necessarily have full rank. In particular, the following cases are distinguished.

Overdetermined system of equations ($m > n$)
By requiring that $[B]$ is

$$h \equiv \|[A]\{x\} = \{b\}\|_2^2 \tag{15}$$

is a minimum, one obtains

$$[A]^T[A]\{x\} = [A]^T\{b\} \tag{16}$$

Therefore, the solution of (1) can be stated as

$$\{x\} = [A]^T\{b\} \tag{17}$$

is the *right pseudo-inverse matrix*.

Undetermined system of equations ($m < n$)
The solution is obtained imposing the minimum of the Euclidean norm

$$g \equiv \|x\|_2^2 \tag{18}$$

with $\{x\}$ subjected to (14). Thus, introducing the new objective function,

$$g' \equiv g + \{x\}^T([A]\{x\} - \{b\}) \tag{19}$$

the solution is achieved solving the system

$$\begin{bmatrix} I & A^T \\ A^T & 0 \end{bmatrix}\begin{bmatrix} x \\ \lambda \end{bmatrix} \tag{20}$$

DOI: 10.1002/tal

or

$$\{x\} = [A]^{+}\{b\} \tag{21}$$

where

$$[A]^{+} = [A]^{T}\left([A][A]^{T}\right)^{-1} \tag{22}$$

is the *left pseudo-inverse matrix*.

4.2 The least-squares method

Since there is abundance of software procedures for computing the least-squares solution of a system of algebraic equations

$$[A]\{x\} = \{b\} \tag{23}$$

the computation of the pseudo-inverse can be reduced to such a solution. These procedures are often based on QR decomposition by means of Householder reflections or GS orthogonalization. Let

$$\begin{aligned} \{b_1\} &= \{1 \quad 0 \quad 0 \quad \cdots \quad 0\}^T \\ \{b_2\} &= \{0 \quad 1 \quad 0 \quad \cdots \quad 0\}^T \\ \{b_3\} &= \{0 \quad 0 \quad 1 \quad \cdots \quad 0\}^T \\ &\vdots \end{aligned} \tag{24}$$

$$\{b_m\} = \{0 \quad 0 \quad 0 \quad \cdots \quad 1\}^T \tag{25}$$

The procedure differs according to the dimensions of $[A]$.

Case $m > n$

(1) Solve m times the system

$$[A]^{T}[A]\{x\} = [A]^{T}\{b\} \tag{26}$$

(2) From the m solutions $\{x_1\}, \{x_2\}, \ldots, \{x_m\}$ one can form the pseudo-inverse matrix

$$[A]^{+} = [\{x_1\} \quad \{x_2\} \quad \{x_2\} \quad \cdots \quad \{x_m\}] \tag{27}$$

Case $n < m$

(1) Solve m times the system

$$\begin{bmatrix} I & A^T \\ A^T & 0 \end{bmatrix}\begin{bmatrix} x \\ \lambda \end{bmatrix} \tag{28}$$

DOI: 10.1002/tal

Also in this case the pseudo-inverse is given by equation (27). The square matrices in (26) and (28) are singular or ill conditioned. Thus their solution requires special care. As mentioned, an appropriate way to solve least-squares problems is by means of GS orthogonalization or Householder QR factorization.

4.3 Greville's method

(1) Decompose the matrix $[A]_{m\times n}$ into row vectors $\{a_i\}$,$(i = 1, 2, \ldots, m)$

$$[A]^+ = \begin{bmatrix} a_1^T & a_2^T & a_3^T & \cdots & a_m^T \end{bmatrix} \tag{29}$$

(2) Let matrix

$$[A_i]_{i\times n} = \begin{bmatrix} A_{i-1} \\ a_i \end{bmatrix} \tag{30}$$

with $[A_1]_{1\times m} = \{a_1\}_{1\times m}$.

(3) For $i = 2, \ldots, m$ compute the matrices $[A]^+$ as

$$[A_i]^+_{n\times i} = [A_{i-1}]^+ \{b_i\}^T \{d_i\} \big| \{b_i\}^T \tag{31}$$

where

$$\begin{gathered} \{d_i\}^+_{1\times(i-1)} = \{a_i\}[A_{i-1}]^+ \\ \{c_i\}_{1\times n} = \{a_i\} - \{d_i\}[A_{i-1}] \\ \{b_i\}_{1\times n} = \frac{\{c_i\}}{\{c_i\}\{c_i\}^T} \; (\|c_i\| \neq 0) \\ \{b_i\}_{1\times n} = \frac{\{d_i\}[A^+_{i-1}]^T}{1+\{d_i\}\{d_i\}^T} \; (\|c_i\| = 0) \\ [A_1]^+ = \frac{\{a_1\}}{\{a_1\}\{a_1\}^T} \; (\|a_1\| \neq 0) \\ [A_1]^+ = a_i \; (\|a_1\| \neq 0) \end{gathered} \tag{32}$$

(4) After m repetitions $[A_m]^+$ gives the pseudo-inverse $[A_m]^+_{m\times n}$ of matrix $[A]$.

5. MODAL TESTING OF CHIMNEY

The height of the studied chimney, w.r.t. ground placed at 4 m above sea level, is 200 m (Figure 2). The building is composed of the following parts:

- An external shell, made of reinforced concrete, with a height of 195·8 m and with diameter of section variable from 23·0 m (at the bottom) to 19·1 m. The foundation is a cylindrical structure (with a diameter of 55·0 m and 3·0 m thickness) and a series of poles (with a diameter of 1 m each) drilled in the ground to a depth of −56·0 m above sea level.
- Four internal flues, with a diameter of 5·0 m each, made of acid-repellent and insulated bricks. Each flue is divided into 10 portions of 17·0 m, except the highest one, which is substantially shorter, and each one is placed on a horizontal platform made of reinforced concrete that distributes the weight to the external shell. At the top of the chimney there is a cover platform at a height of 197·0 m.

DOI: 10.1002/tal

Figure 2. Chimney

The material of the chimney is isotropic with Young's modulus $E = 36\,\text{GPa}$, density $\rho = 1500\,\text{kg/m}^3$ and Poisson coefficient $\nu = 0{\cdot}2$.

Experimental tests for measurement of the dynamic response of the chimney have been performed using a shaker. The shaker used is a low-frequency-range machine (ISMES BF50/5), with the following features:

- maximum amplitude of generated force: 50 KN;
- maximum frequency of generated force: 5 Hz;
- structural mass (without inertial masses): 1840 kg.

The shaker has been placed at the top of chimney. At a position of 197·0 m a.s.l. the shaker excited the chimney by means of a sinusoidal load with variable frequency, along two orthogonal directions (Cavacece and Valentini, 2003). The response of the structure has been monitored at 30 different locations along the chimney. In particular, the 22 piezoelectric accelerometers and eight eight-dynamical seismometers have the following features:

- accelerometer type: Endeveco mod. 2262C-25; frequency response: linear from 0 up to 500 Hz; sensitivity: 9·81 cm/s/V;
- seismometer type: Teledyne mod.Geotech S-13; frequency response: linear from −1 up to 50 Hz; sensitivity: 0·00170 cm/s/V.

The experimental setup allows us to measure circular frequencies of damped oscillation and transmissibility functions. The measured circular frequencies of damped oscillation are summarized in Table 1. Natural circular frequencies ω_r are obtained by the finite element method (Cavacece and Valentini, 2003) (Table 2). The model of chimney has been meshed using four-node standard shell elements with 5 d.o.f. per node. Referring to Table 3, we can calculate $\sqrt{\omega_r^2 - \omega_{E_{r,q}}}$, right side of system (7) with $N_r = N_q = 3$.

DOI: 10.1002/tal

Table 1. Experimental circular frequencies of damped oscillation

rth mode	$\omega_{E_{r,1}}$ (rad/s)	$\omega_{E_{r,2}}$ (rad/s)	$\omega_{E_{r,3}}$ (rad/s)
1	1·2	1·213	1·238
2	10·04	10·034	10·022
3	21·960	21·953	21·972

Table 2. Natural circular frequencies

rth mode	ω_r (rad/s)
1	1·257
2	10·053
3	22·054

Table 3. Right side of system

rth mode	$2\sqrt{\omega_r^2 - \omega_{Er,q}^2}$ (rad/s)	$2\sqrt{\omega_r^2 - \omega_{Er,q}^2}$ (rad/s)	$2\sqrt{\omega_r^2 - \omega_{Er,q}^2}$ (rad/s)
1	0·748	0·659	0·435
2	1·022	1·235	1·577
3	4·068	4·216	3·800

Table 4. Experimental values of frequency response

qth measure	Frequency (Hz)	Frequency response ($ms^{-2}N^{-1}$)
1	0·01	$\Re[H] = 0{\cdot}01$
2	0·1597	$\Im[H] = +0{\cdot}25$
3	0·194	$\Im[H] = -0{\cdot}72$
4	3·0	$\Im[H] = -0{\cdot}0001$
5	3·495	$\Im[H] = -0{\cdot}1$

The transmissibility functions have been computed for the nodal displacement at measurement locations. Experimental analysis leads to the values of the real part $\Re[H(f)]$ and of the imaginary part $\Im[H(f)]$ of the frequency response at the top of the chimney. Experimental results of the frequency response at the top of the chimney have been evaluated referring to the values of frequency in Table 4.

6. COMPLETE MODAL DATA

Let us suppose that the modal data are complete in terms of the number of measured modes. For this application we have an overdetermined system of equations, where the number of equations $m = 9$ is greater than the number of unknowns $n = 2$. Referring to Table 3, system (7), with $N_r = N_q = 3$, provides the following solutions:

DOI: 10.1002/tal

Table 5. Circular frequencies of damped oscillation and modal damping ratio

rth mode	ω_{d_r} (rad/s)	ζ_r
1	1·219	$2{\cdot}366 \times 10^{-1}$
2	10·032	$6{\cdot}453 \times 10^{-2}$
3	21·962	$9{\cdot}113 \times 10^{-2}$

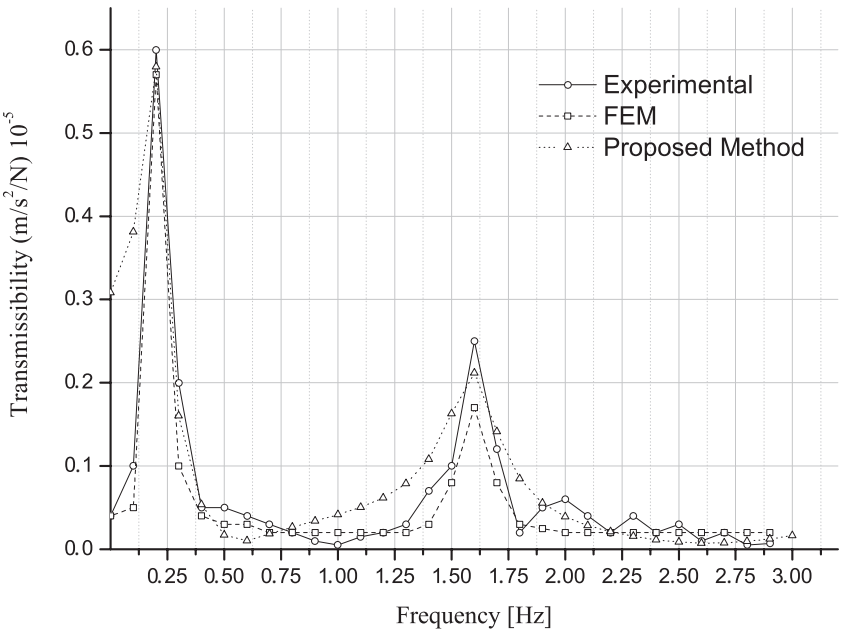

Figure 3. Transmissibility function

$$\alpha = 0{\cdot}583, \quad \beta = 7{\cdot}065 \times 10^{-3} \tag{33}$$

Damped oscillation frequencies and modal damping ratios are summarized in Table 5.

6.1 Modal shapes

Substituting modal damping ratio ζ_r (Table 5) and those of frequency response (Table 4) into system (11), we obtain the following solutions:

$$(X_T^2)_1 = 0{\cdot}432, \quad (X_T^2)_2 = 2{\cdot}746, \quad (X_T^2)_3 = 3{\cdot}744 \tag{34}$$

at the top of chimney ($i = k = T$) by means of the pseudo-inverse matrix (Figure 1).

In Figure 3 transmissibility functions obtained by the proposed methodology, experimental results and FEM ones are compared. Figure 4 shows the real and imaginary parts of the transmissibility fucntion deduced by the pseudo-inverse matrix. Referring to Table 6, elapsed CPU time obtained by proposed methods is compared.

DOI: 10.1002/tal

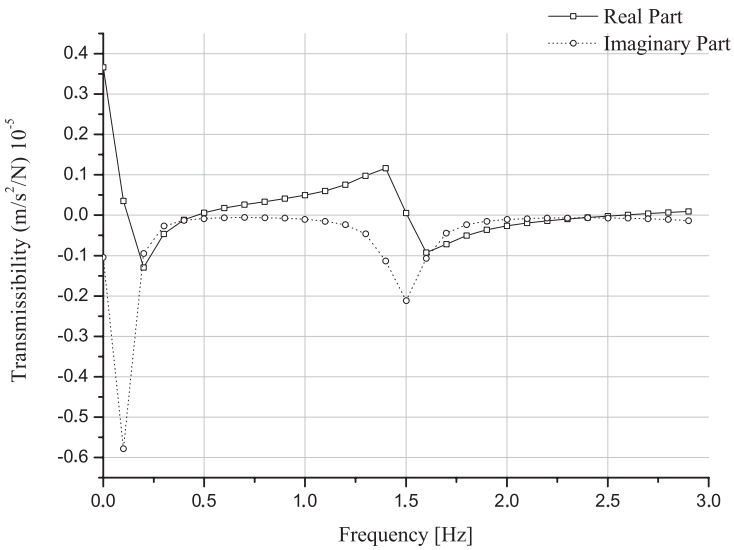

Figure 4. Real and imaginary parts of the transmissibility function

Table 6. CPU time

Method	CPU (time ratios)
Least squares Householder	1·0
Least squares Gram–Schmidt	2·0
Greville's method	3·0

7. INCOMPLETE MODAL DATA

Let us suppose that the modal data are incomplete only in terms of the number of measured modes. If there is noise, structural identification will be ill posed. In this context, the word *noise* has wide implications, as for example: any causal or random factors which should not or cannot be modelled; further information is not available; some information of the system has been lost; some vibration data cannot be analysed; the modal data are incomplete in terms of the number of measured modes.

When the second mode of the eigensolution is omitted, we have an overdetermined system of equations, where the number of equations $m = 6$ is greater than the number of unknowns $n = 2$. Referring to Table 3, we obtain the following solutions:

$$\alpha = 0{\cdot}602, \quad \beta = 7{\cdot}037 \times 10^{-3} \tag{35}$$

Damped oscillation frequencies and modal damping ratios are summarized in Table 7.

8. CONCLUSIONS

The generalized inverse, an elegant mathematical technique, provides only one solution to solve an overdetermined problem with or without noise. In this paper, the application of the generalized inverse allows us to determine modal damping ratios and modal shapes of a chimney.

DOI: 10.1002/tal

Table 7. Circular frequencies of damped oscillation and modal damping ratio for incomplete modal data

rth mode	ω_{d_r} (rad/s)	ζ_r
1	1·219	$2{\cdot}438 \times 10^{-1}$
2	10·032	$6{\cdot}529 \times 10^{-2}$
3	21·962	$9{\cdot}124 \times 10^{-2}$

Table 8. Modal damping ratio

rth mode	Complete modal data ζ_r	Incomplete modal data ζ_r	Error (%)
1	$2{\cdot}366 \times 10^{-1}$	$2{\cdot}438 \times 10^{-1}$	3·0
2	$6{\cdot}453 \times 10^{-2}$	$6{\cdot}529 \times 10^{-2}$	1·1
3	$9{\cdot}113 \times 10^{-2}$	$9{\cdot}124 \times 10^{-2}$	0·1

Table 9. Symbols

Symbol	Description
$[m]$	Mass(inertia) matrix
$[c]$	Damping matrix
$[k]$	Stiffness matrix
α, β	Rayleigh damping coefficients
$\{y\}$	Displacement response vector
$\{F(t)\}$	Forcing excitation vector
$q = 1, 2, \ldots, N_q$	Measure
$r = 1, 2, \ldots, N_r$	Modal shape
$(X_i X_k)_r$	rth modal shape at response location i and excitation location k
f	Frequency
ω_r	rth natural circular frequency
f_r	rth natural frequency
ω_{d_r}	rth circular frequency of damped oscillation
f_{dr}	rth frequency of damped oscillation
$\omega_{E_{r,q}}$	Experimental circular frequency, acquired for measure q and mode r
ζ_i	Modal damping ratio for the ith normal mode
$[H(s)]$	Transfer function matrix
S	Laplace variable: $j\omega = j2\pi f$ in frequency domain

The investigation is divided into two parts. In the first part, we determine the modal damping ratios assuming Rayleigh damping. In the second part, the modal shapes and frequency response of displacement are computed. It is shown that Rayleigh damping can predict accurately the response of a chimney in a large frequency range, because the chimney has a symmetrical structure and the material of the chimney has linear elastic properties.

The generalized inverse, a very useful tool in linear matrix theory, has the following features:

(1) By using an overdetermined system of equations with complete modal data, we obtain modal damping ratios. In addition, the acquired signals and computed results of frequency response of displacement show good agreement.
(2) When the second mode of the eigensolution is omitted, the physical parameters, obtained by using the generalized inverse method, are quite similar to those obtained by using an overdetermined system of equations with complete modal data (Table 8). Therefore, the generalized inverse method minimizes the effect of noise in this mechanical system.

DOI: 10.1002/tal

(3) Application of the generalized inverse method in structural identification is not completely successful using a set of simultaneous equations which is undetermined.

Finally, the generalized inverse method is a means for determining the least-squares solution of a set of simultaneous equations which is overdetermined. We demonstrate that this method leads to reliable results for modal damping ratios of a chimney with negligible damping. In fact, the response of the chimney obtained by this method shows good agreement with the experimental response of the chimney subjected to a generic wind periodic excitation and the response obtained by the finite elements method.

ACKNOWLEDGEMENTS

The authors wish to acknowledge Professor Ettore Pennestrì for his helpful advice during the development of this work.

REFERENCES

Adhikari S, Woodhouse J. 2001. Identification of damping: Part 1. Viscous damping. *Journal of Sound and Vibration* **243**(1): 43–61.

Cavacece M, Valentini PP. 2003. An experimental and numerical approach to investigate the dynamic response of a four-flue chimney of a thermoelectrical-electrical plant. *Structural Design of Tall and Special Buildings* **12**: 283–291.

de Silva CW. 2000. *Vibration Fundamentals and Practice*. CRC Press: New York.

Dovstam K. 1997. Receptance model based on isotropic damping function and elastic displacement model. *International Journal of Solids and Structures* **34**(21): 2733–2754.

Ewins DJ, Gleeson PT. 1982. A method for modal identification of lightly damped structures. *Journal of Sound and Vibration* **84**(1): 57–79.

Gaylard ME. 2001. Identification of proportional and other sorts of damping matrices using a weighted response: integral method. *Mechanical Systems and Signal Processing* **15**(2): 245–256.

He J, Fu Z-F. 2004. *Modal Analysis*. Butterworth Heinemann: Oxford.

Lagomarsino S. 1993. Forecast models for damping and vibration periods for duildings. *Journal of Wind Engineering and Industrial Aerodynamics* **48**: 221–239.

Lee S-H, Min K-W, Hwang J-S, Kim J. 2004. Evaluation of equivalent damping ratio of a structure with added dampers. *Engineering Structures* **26**: 335–346.

Liu K, Kujath MR, Zheng W. 2001. Evaluation of damping non-proportionality using identified modal information. *Mechanical Systems and Signal Processing* **15**(1): 227–242.

Luk WL. 1987. Identification of physical mass, stiffness and damping matrices using pseudo-inverse. In *5th International Modal Analysis Conference*; 679–685.

Mohammad DR, Khan NU, Ramamurti V. 1995. On the role of Rayleigh damping. *Journal of Sound and Vibration* **185**(2): 207–218.

Pennestri E, Cheli F. 2006. *Cinematica e Dinamica dei Sistemi Multibody*. 1. Casa Editrice Ambrosiana: Milan.

Prells U, Friswell MI. 2000. A measure of non-proportional damping. *Mechanical Systems and Signal Processing* **14**(2): 125–137.

Singiresu SR. 2004. *Mechanical Vibrations.* Pearson Education: Singapore.

To WM, Ewins DJ. 1995. The role of the generalized inverse in structural dynamics. *Journal of Sound and Vibration* **186**(2): 185–195.

Trombetti T, Silvestri S. 2006. On the modal damping ratios of shear-type structures equipped with Rayleigh damping systems. *Journal of Sound and Vibration* **292**: 21–58.

Watanabe Y, Isyumov N, Davemport AG. 1997. Empirical aerodynamic damping function for tall building. *Journal of Wind Engineering and Industrial Aerodynamics* **72**: 313–321.

DOI: 10.1002/tal